

Silica nanomachining using laser plasma soft x rays

Tetsuya Makimura,^{a)} Satoshi Uchida, and Kouichi Murakami
Institute of Applied Physics, University of Tsukuba, Tsukuba, Ibaraki 305-8573, Japan

Hiroyuki Niino
Photonics Research Institute, National Institute of Advanced Industrial Science and Technology, Tsukuba, Ibaraki 305-8565, Japan

(Received 29 December 2005; accepted 24 July 2006; published online 7 September 2006)

In order to demonstrate silica nanomachining, the authors fabricated line-and-space contact masks with spaces of 53 and 70 nm on silica glass plates, followed by irradiation with laser plasma soft x rays (LPSXs) with wavelengths around 10 nm. Trenches with the narrowest width of 54 nm and an aspect ratio of ~ 1 were fabricated by the LPSX irradiation through the contact masks. It was also clarified that silica glass can be machined by irradiation with LPSXs in the wavelength range of 6–30 nm in Ar gas which was used as an x-ray bandpass filter. © 2006 American Institute of Physics. [DOI: 10.1063/1.2347117]

Nanomachining of silica glass can be applied to the fabrication of nanometric chemical analyzers and chemical reactors in medicine and biotechnology,^{1,2} of molds used in nanoimprint,^{3,4} and of optical devices such as gratings, photonic crystals, and optical waveguides. In the previous letter, we reported a single-step technique that can be used for micromachining of silica glass for these applications.⁵ In this technique, silica surfaces are ablated by irradiation with laser plasma soft x rays (LPSXs), which are generated using a conventional pulsed Nd:YAG (yttrium aluminum garnet) laser. In the letter, we demonstrated the following features of LPSXs. (a) The intensity of a single pulse of LPSXs is sufficiently high to ablate silica. (b) A silica glass surface with a radius of 200 μm can be ablated at 45 nm/shot. (c) Maskless single-step processing can be easily achieved. (d) Despite the spatial beam quality of the laser beam, that of LPSXs is sufficiently high to realize micromachining without the use of a beam homogenizer. These features enable us to realize a novel nanomachining technique as well as a practical, low-cost micromachining technique.

To date for silica micromachining, techniques such as electron beam lithography,^{3,4,6–9} photolithography,¹⁰ and focused ion-beam etching¹¹ have achieved high-resolution features with dimensions of less than 1 μm . Although nanomachining has been achieved, the above techniques suffer some inherent difficulties. These techniques involve multiple and time-consuming process steps, and only a limited number of materials suitable for etchants and resists are available. Compared to these techniques, photomachining (i.e., direct laser machining) is promising because it is suitable for mass production and it only involves a single direct process.^{5,12–18} Further, photomachining with a resolution of ~ 10 nm requires soft x rays, since the ultimate resolution is limited by the diffraction limit.

One of the most important features of LPSXs is their potential capability for nanomachining with a resolution of the order of 10 nm. However, the nanoscale resolution still needs to be demonstrated. In particular, a resolution of 10 nm may not be achievable due to factors such as the thermal diffusion length of ~ 77 nm in silica glass during

7 ns LPSX irradiation.⁵ Smoothing due to thermal diffusion might result in dull structures. In the present letter, we demonstrate that silica nanomachining can be achieved using nanosecond LPSXs.

Figure 1(a) shows the experimental setup. The details of the setup are given elsewhere.⁵ Silica glass (synthetic quartz glass) plates (Q) were irradiated with pulsed LPSXs (X) in a vacuum chamber at a pressure of 2×10^{-4} Pa, through the windows of nanoscale contact masks (M), using a focusing ellipsoidal mirror (E).

The LPSXs were generated by the irradiation of rotating Ta targets (T) with 532 nm Nd:YAG laser light (Y) with a pulse duration of 7 ns. The laser light has an energy of 700 mJ/pulse and an estimated fluence of $\sim 1 \times 10^4$ J/cm² at the targets. The Ta laser plasma emits soft x rays in the energy range of 10–300 eV.⁵ It is noted that the LPSX pulses have the same pulse duration as that of the Nd:YAG laser light pulses. The irradiation of Ta targets with Nd:YAG laser light also results in emission of particles (p) such as plasma, ions, electrons, and liquid debris with a diameter of ~ 1 μm from the targets. In order to prevent damage to the

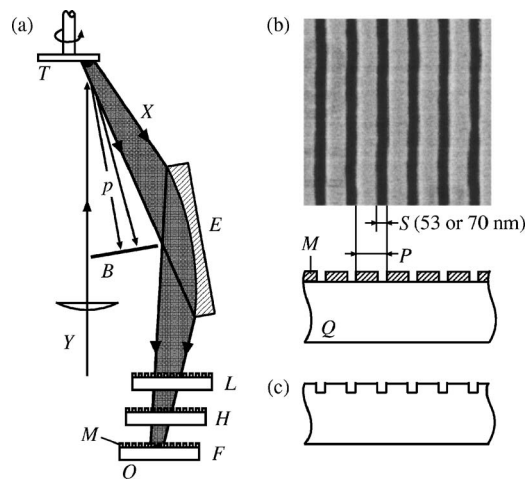


FIG. 1. (a) Experimental setup for silica nanomachining using LPSXs. (b) SEM image of a line-and-space contact mask (M) fabricated on a silica plate (Q). (c) Silica glass plate after irradiation with LPSXs and removal of the contact mask.

^{a)}Electronic mail: makimura@ims.tsukuba.ac.jp

samples and contamination from the particles, a blocking plate (*B*) was placed between the targets and the samples. The LPSXs were focused using an ellipsoidal mirror coated with a Au layer (*E*). The mirror was designed such that it could efficiently focus LPSXs around 10 nm. Since the mirror reflects LPSXs lower than ~ 200 eV, only LPSXs lower than ~ 200 eV were focused on the samples.

To attain nanoscale patterning, WSi line-and-space mask (*M*) were fabricated on silica glass plates by standard electron beam lithography, which involved (1) deposition of WSi films with a thickness of 80 nm by dc sputtering, (2) spin coating of resist layers, (3) exposure of the resists to a scanning electron beam, (4) development of the resists, (5) reactive ion etching of the WSi films through windows in the resist masks, and (6) ashing of the resists. As shown in Fig. 1(b), two kinds of WSi contact masks (*M*) were fabricated. The masks have spaces (*S*) of either 53 or 70 nm and a pitch (*P*) of 175 nm.

In order to change the fluence of the LPSXs without changing the spectrum of LPSXs, the samples were placed at two different positions, *L* and *H*, away from one of the focal points of the mirror (*F*) by distances of 3.0 and 4.5 mm, respectively, as shown in Fig. 1(a). At position *H*, the LPSX fluence is so intense that the central part of the WSi mask was damaged by a single shot of LPSX irradiation. At position *L*, the LPSX fluence was sufficiently low and no damage on the WSi mask was observed even after 200 shots of LPSX irradiation.

After the silica glass plates were irradiated with the LPSXs through the windows of the WSi masks, the masks were selectively removed by reactive ion etching using SF_6 gas for 6.7 min. A WSi film is etched at a rate of 170 nm/min, while silica glass is etched at 9.7 nm/min at most.

The nanostructures fabricated on the silica glass plates, as illustrated in Fig. 1(c), were then observed using a scanning electron microscope (SEM). Figure 2(a) shows a cross-sectional SEM image of a series of trench structures that were fabricated on a silica plate by 70 shots of LPSX irradiation through the 53 nm windows of the WSi mask at the low fluence position *L*. The trenches have widths (*W*) of 54–81 nm and depths (*D*) of 50–80 nm. Figure 2(b) shows a cross-sectional SEM image of a series of trench structures that were fabricated by a single shot of LPSX irradiation through a WSi mask with 70 nm windows at the high fluence position *H*. The trenches have widths of 79–84 nm and a depth of ~ 30 nm. We should emphasize that nanomachining can be achieved by LPSX irradiation.

The fabricated trenches are wider than the original windows in the masks. This is possibly a result of the ablation process that the edges of the WSi masks are ablated together with the silica surface layers even at the low fluence.

We performed the following two experiments to demonstrate that the fabricated structures were solely due to LPSX irradiation and not due to ion etching of the silica surface during the fabrication process or removal process of WSi masks. In one experiment, a WSi mask with window widths of 50–200 nm and a thickness of 80 nm was fabricated on a silica plate and the mask was removed by reactive ion etching without LPSX irradiation. As a result, no structure on silica surface deeper than 5 nm was observed using an atomic force microscope. Furthermore, the silica surface in

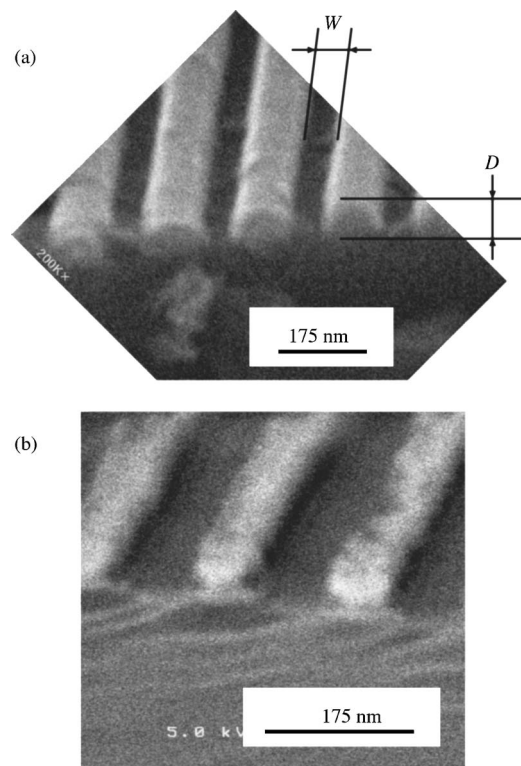


FIG. 2. Cross-sectional SEM images of trenches fabricated by LPSX irradiation (a) at low fluence for 70 shots and (b) at high fluence for a single shot.

the window of WSi mask is estimated to be etched by 4.6 nm at most, during the period of 28 s for the 80-nm-thick WSi mask to be completely etched. After the complete removal of the mask, the nanostructured silica surface is etched uniformly. These results reveal that the nanostructures shown in Fig. 2 are mainly induced by LPSX irradiation.

In the other experiment, a silica plate was irradiated with LPSXs through a Ni contact mask with square apertures with a size of $8 \mu\text{m}$ for ten shots at an ablation rate of 10 nm/shot. After removing the Ni mask, the WSi mask with a thickness of $5 \mu\text{m}$ and a window width of 1.5 mm was fabricated on the silica plate and was removed by the reactive ion etching. Thus, some of the LPSX-fabricated holes were directly exposed to the etching plasma, while the others were covered with the WSi film. After removing the WSi mask, the square holes were clearly observed using a confocal microscope (Keyence Corp., VK-8510). The depths are 97 ± 7 and 95 ± 7 nm for the holes covered with and without the WSi film, respectively, during the removal process. This result reveals that silica etching during the removal process is not enhanced even if a silica plate is irradiated with LPSXs before the removal process. That is, LPSX irradiation does not cause damage that is sensitive to the ion etching. Consequently, the fabricated structures shown in Fig. 2 were mainly due to LPSX irradiation.

In order to realize nanomachining, it is necessary to demonstrate ablation by LPSXs with a wavelength of ~ 10 nm because the precision is limited by the diffraction limit. To select a particular spectral region of the generated LPSXs, the vacuum chamber was filled with Ar gas with a purity of 99.9995% as a soft x-ray filter. For this measurement, synthetic quartz glass plates were placed at the focal point *F* and were irradiated with LPSXs through $8 \mu\text{m}$

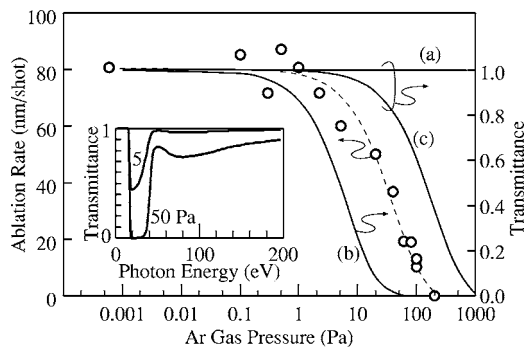


FIG. 3. Ablation rate (open circles) of silica glass by LPSX irradiation in Ar gas. The inset shows transmittance spectra of Ar gas at 5 and 50 Pa. Curves (a), (b), and (c) show transmittance of Ar gas at 10, 20, and 100 eV, respectively, as a function of Ar gas pressure.

square apertures in a Ni contact mask. After LPSX irradiation, the ablation depth was measured using the confocal microscope.

The circles in Fig. 3 indicate ablation rate of silica glass in Ar gas as a function of gas pressure. The rate decreases as pressure increases in the range of 1–100 Pa. The inset in Fig. 3 shows the reported transmittance spectra of Ar gas at given pressures with a path length of 150 mm at room temperature.¹⁹ The spectra can be divided into three regions: (i) a transparent region below 15 eV, (ii) a strong absorption band in the region of 15–40 eV, and (iii) a weak absorption band above 40 eV. The solid lines in Fig. 3 show the transmittance at (a) 10 eV, (b) 20 eV, and (c) 100 eV, which are the typical photon energies of the three regions. Ablation is not caused by irradiation with LPSXs below 15 eV, because the ablation depth decreases with pressure while the intensity of LPSXs below 15 eV remains constant. In addition, the irradiation of LPSXs between 15 and 40 eV is not always necessary for ablation, because ablation occurs in Ar gas at 50 Pa, despite the complete elimination of the LPSXs between 15 and 40 eV. As noted above, only LPSXs below 200 eV are focused on the silica plates. Therefore, it can be concluded that only LPSXs in the range of 40–200 eV (6–30 nm) can cause the ablation of silica glass. Thus, the results shown in Fig. 3 reveal the capability of silica nanomachining.

Thermal heating of the lattice occurs during the relaxation process of the electrons and holes in the energy bands. The energy accumulated during LPSX irradiation is almost comparable to that required to evaporate the silica surface.⁵ Therefore, heating beyond the boiling point might be one of the possible processes resulting in the ablation of silica surfaces. However, the thermal diffusion length during LPSX irradiation has been estimated to be 77 nm during LPSX irradiation from the thermodynamic parameters at room temperature.⁵ It is impossible to explain the clear 50 nm trench structures only by the thermal heating model, because the structures must become dull at the extent of the diffusion length. Therefore, the LPSX ablation of silica is caused by

other mechanisms such as Coulomb explosion and explosive desorption due to multiple holes generated in the valence band by LPSX irradiation, besides the thermal effect.

In conclusion, we have investigated silica nanomachining using LPSXs with wavelengths around 10 nm. In order to demonstrate nanomachining, we fabricated line-and-space contact masks with spaces of 53 and 70 nm on silica glass plates. By irradiation with white LPSXs through contact masks, trenches were clearly fabricated. In the case of the 53 nm mask, the trenches were 54–81 nm wide and 50–80 nm deep. In the case of the 70 nm mask, the trenches were 79–84 nm wide and ~30 nm deep. To clarify the photon-energy range of LPSXs that can ablate silica glass, silica glass was irradiated with LPSXs in Ar gas as an x-ray bandpass filter. Silica glass can be ablated by irradiation with LPSXs in the range of 40–200 eV (6–30 nm). We have thus demonstrated a nanomachining technique using LPSXs.

The authors would like to thank K. Kondo for help with developing the experimental apparatus, H. Ohkubo for SEM observations, K. Asakawa for providing the experimental facility, and S. Aoki for helpful discussions on x-ray optics and for optical microscope observations. This work was partially supported by Industrial Technology Research Grant Program in 2005 from NEDO of Japan and JSPS Kakenhi.

- ¹J. Han, S. W. Turner, and H. G. Craighead, *Phys. Rev. Lett.* **83**, 1688 (1999).
- ²N. Kaji, Y. Tezuka, Y. Takamura, M. Ueda, T. Nishimoto, H. Nakanishi, Y. Horiike, and Y. Baba, *Anal. Chem.* **76**, 15 (2004).
- ³S. Y. Chou, P. R. Krauss, and P. J. Renstrom, *Science* **272**, 85 (1996).
- ⁴S. Y. Chou, C. Keimel, and J. Gu, *Nature (London)* **417**, 835 (2002).
- ⁵T. Makimura, H. Miyamoto, Y. Kenmotsu, K. Murakami, and H. Niino, *Appl. Phys. Lett.* **86**, 103111 (2005).
- ⁶D. M. Tennant, T. L. Koch, P. P. Mulgrew, R. P. Gnall, F. Ostermeyer, and J.-M. Verdiell, *J. Vac. Sci. Technol. B* **10**, 2530 (1992).
- ⁷C. Dix, P. F. McKee, A. R. Thurlow, J. R. Towers, and D. C. Wood, *J. Vac. Sci. Technol. B* **12**, 3708 (1994).
- ⁸D. R. Allee, C. P. Umbach, and A. N. Broers, *J. Vac. Sci. Technol. B* **9**, 2838 (1991).
- ⁹D. Winkler, H. Zimmermann, M. Mangerich, and R. Trauner, *Microelectron. Eng.* **31**, 141 (1996).
- ¹⁰I. Benninon, D. C. J. Reid, C. J. Rowe, and W. J. Steward, *Electron. Lett.* **22**, 341 (1986).
- ¹¹J. Albert, K. O. Hill, B. Malo, D. C. Johnson, F. Bilodeau, I. M. Templeton, and J. L. Brebner, *Appl. Phys. Lett.* **63**, 2309 (1993).
- ¹²J. Ihremann, B. Wolf, and P. Simon, *Appl. Phys. A: Solids Surf.* **54**, 363 (1992).
- ¹³K. Sugioka, S. Wada, H. Tashiro, K. Toyoda, Y. Ohnuma, and A. Nakamura, *Appl. Phys. Lett.* **67**, 2789 (1995).
- ¹⁴J. Zhang, K. Sugioka, T. Takahashi, K. Toyoda, and K. Midorikawa, *Appl. Phys. A: Mater. Sci. Process.* **71**, 23 (2000).
- ¹⁵J. Zhang, K. Sugioka, and K. Midorikawa, *Opt. Lett.* **23**, 1486 (1998).
- ¹⁶J. Wang, H. Niino, and A. Yabe, *Appl. Phys. A: Mater. Sci. Process.* **68**, 111 (1999).
- ¹⁷J. Wang, H. Niino, and A. Yabe, *Appl. Phys. A: Mater. Sci. Process.* **69**, S271 (1999).
- ¹⁸T. Makimura, S. Mitani, Y. Kenmotsu, K. Murakami, M. Mori, and K. Kondo, *Appl. Phys. Lett.* **85**, 1274 (2004).
- ¹⁹B. L. Henke, E. M. Gullikson, and J. C. Davis, *At. Data Nucl. Data Tables* **54**, 181 (1993).